

**22****RESPIRATORY PROTECTIVE DEVICE DESIGN USING  
CONTROL SYSTEM TECHNIQUES**

William A. Burgess, Harvard School of Public Health,  
and Donald Yankovich, Charles Stark Draper Laboratory  
Massachusetts Institute of Technology

**INTRODUCTION**

In reviewing the history of respiratory protection, one finds that developments up to 1950 resulted in a variety of air-purifying, supplied-atmosphere, and self-contained respiratory protective devices (RPDs). Since 1950, the RPD designs have been relatively static mainly because neither the military nor the commercial designer has had a rational design base available for use. We have explored the feasibility of a control system analysis approach to provide such a design base that will benefit all sectors interested in vigorous RPD design evolution.

A system design approach requires that all functions and components of the system be mathematically identified in a model of the RPD. The mathematical notations must describe the operation of the components as closely as possible. The individual component mathematical descriptions are then combined to describe the complete RPD. Finally, analysis of the mathematical notation by control system theory is used to derive compensating component values that force the system to operate in a stable and predictable manner. As a further step, optimal control theory may be applied to obtain an optimally designed system. This system design procedure permits the designer to work with quantitative values for the system parameters prior to building the system. He can consider simplification, improvement of the system, and cost reduction before prototypes are constructed.

A mathematical description of the RPD is the basis of its system design. From such a system model the designer can calculate those parameters or characteristics for which the model has been developed as a function of the mechanical characteristics of the RPD.

**SUBSYSTEMS AND NOMENCLATURE**

The first step in the modeling process was to break the RPD into subsystems and then into individual components. RPD system models will be generated by properly combining models of these small subsystems. A nomenclature for systems and subsystems is given in table 22.1.

There are four major subsystems in a RPD system: the mask, the air delivery system, the environmental maintenance system, and the communications system. The mask is a respiratory enclosure that covers at least the nose and mouth or is held in the mouth. It is a mechanical barrier to a hostile environment and includes all parts of the "facepiece" except valves and external air passages. (Internal air passages are considered resistances and are lumped together with port resistance.)

The air delivery system (ADS) is made up of valves, external air passages, and valve control systems. Valve control can be either pneumatic or electronic.

**Table 22.1** *Respiratory protective device (RPD).*

<i>Mask</i>	<i>Air delivery system (ADS)</i>	<i>Environmental maintenance system (EMS)</i>	<i>Communications</i>
Seals	Electronic control subsystem (ECS <sup>2</sup> )	Environment supply subsystem (ESS <sup>2</sup> ) Tank Heat exchanger	Diaphragm
Suspension system	Air passage subsystem (APS <sup>2</sup> )	Pressure and venting subsystem (PVS <sup>2</sup> ) Regulator Pressure supplementary source	Electronic
Envelope	Valve control subsystem (VCS <sup>2</sup> ) Valves Control system	Air reconditioning subsystem (ARS <sup>2</sup> ) H <sub>2</sub> O removal CO <sub>2</sub> scrubber Heat exchanger	
Eyepiece		Filters	
Ports			

The environmental maintenance system (EMS) consists of the components that supply air, filter air, or process air. It has four major subsystems: environmental supply, pressure regulating and venting, filtering, and air reconditioning. With the summation of these subsystems as generalized models, any RPD system can be mathematically constructed.

Models of present RPD systems were constructed by drawing mathematical analogies with electrical systems. This required that RPD systems be made up of effects such as resistance, compliance (capacitance), and inertance (inductance). The state variables of these models therefore were gas pressure and flow.

Resistance is a restriction to gas flow and is primarily due to ports, filters, and air passages. Compliance encompasses those characteristics of the RPD system that allow for gas "storage" including RPD component expansion and gas compression. Inertance is directly related to the same characteristics that cause compliance coupled with the effect of mass. As the system expands or the gas compresses there is an increase in internal pressure that tends to maintain gas flow should a change in flow direction be attempted, hence the analogy to electrical inductance.

Diodes, pressure sources, and flow sources are added to complete the list of component analogies used to model the RPD. Diodes allow flow in only one direction and are primarily used to model the nonlinear behavior of valves, regulators, and seals. Pressure sources are direct analogies to voltage sources and have the property of supplying a constant pressure across any impedance to current flow. Flow sources supply a constant flow through any impedance.

## RESISTANCE (R)

The apparatus described in figure 22.1 was used to measure resistance with a unidirectional blower for the flow source and  $Q_{out}$  removed. Tests for  $R$  were conducted for both inhalation and exhalation. For inhalation tests the exhalation ports were sealed and visa versa. Pressure in the mask was measured with a static probe mounted on the middle of the mannequin forehead for flows of up to 3 liters/sec. Resistance is defined as

$$R = \frac{dP}{dQ_{in}} \quad [\text{cm H}_2\text{O}/(\text{liters}/\text{sec})]$$

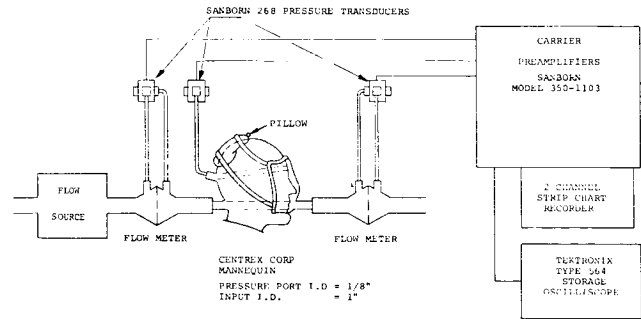


Figure 22.1 Test apparatus used to obtain RPD parameters.

## CAPACITANCE (C)

For the capacitance measurements both flow meters in figure 22.1 were removed and all valves and ports were sealed except for two ports. One port was used to monitor pressure in the mask and the other was connected to a 5 cc syringe. The syringe was used to provide both negative and positive changes in volume by 1 cc increments ( $dV$ ), and the pressure change ( $dP$ ) was monitored. The capacitance can be found from

$$C = \frac{dV}{dP} \quad [\text{cm}^3/\text{cmH}_2\text{O}]$$

If the mask were rigid, the pressure change would be equal to

$$dP = \left( \frac{dV}{\text{volume of mask}} \right) \quad (\text{Pressure absolute}) = \frac{1 \text{ cm}^3 \times 1033.6 \text{ cmH}_2\text{O}}{\text{volume of mask}}$$

If the mask was not rigid, then the pressure change would not be as great and the value of capacity would be greater. Actual measurements on masks gave values six times greater than that calculated for a rigid mask.

## INERTANCE (I)

A method for obtaining  $I$  is to use an oscilloscope to observe the pattern formed by driving the X axis with the pressure transducer connected to the static pressure tap at the input to the mannequin and the Y axis with the pressure transducer connected to the static pressure tap at the forehead of the mannequin. The resonating frequency (the frequency at which the mask was vibrating with its maximum excursion) occurs when the pressure at the input of the mannequin is  $90^\circ$  out of phase with the pressure inside the mask.

Knowing the lowest resonant frequency allows one to calculate the value of  $I$  from the relationship

$$\omega = 2\pi f = \frac{1}{\sqrt{IC/1000}} \quad \text{or} \quad I = \frac{1}{4\pi^2 f^2 C/1000}$$

if damping is ignored.

When the first attempt was made to measure the resonant frequency in this manner, several extraneous resonant frequencies were found near the resonant frequency of the mask. To isolate the undesirable resonances, the mask was damped with weights. Now the low resonances were located and by shortening up various pieces of connecting tubing, they were eliminated or shifted to higher frequencies away from the mask resonance.

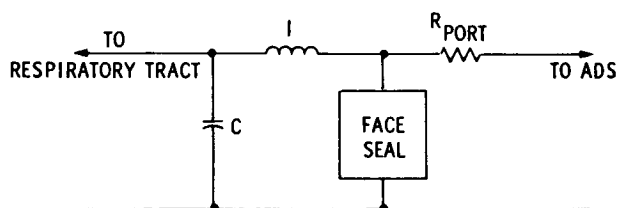
Resonant frequencies were found with the valves removed and ports open. In all cases they were at relatively high frequencies that indicated extremely low values of  $I$ . Then the ports were sealed and much lower resonant frequencies resulted. The ports were then unsealed and with the valves in place the same low resonant frequency occurred as with the ports sealed. The actual frequency depended somewhat on the level of pressure in the mask. The frequency increased at lower pressure levels towards the slightly higher values found with the mask sealed up, as might be expected. All testing was done with dry exhalation valves. The value of  $I$  used for the model was that determined with the valves in place.

### MASK MODEL

Since there are pressure gradients throughout the mask void, the mask can be modeled by a distributed parameter system. Since in most applications the various pressure gradients throughout a mask are small, mask pressure can be assumed uniform throughout the mask void and the mask model reduces to the lumped parameter system of figure 22.2

Also, if the inhalation and exhalation ports are not sealed the port resistance is shorted to the return and the resulting system is governed by a second order equation.

Two first order equations thus describe the mask pressure-flow relationships



$$\dot{P} = \frac{1}{C} (q_s - Q)$$

$$\dot{Q} = \frac{1}{I} (P - QR)$$

Figure 22.2 Mask model showing facial seal model location.

$$\dot{P} = \frac{1}{C} (q_s - Q)$$

$$\dot{Q} = \frac{1}{I} (P - QR)$$

### CONTAMINANT LEAKAGE

Modeling of the mask must include the seal, which is the interface between the user's face and the respirator system. Inevitably, seals are subject to leakage between the controlled atmosphere within the respirator and the outside contaminated environment. The magnitude of this leakage is acceptably small at normal mask operating conditions; however, if mask pressure relative to ambient becomes sufficiently large, the mask seal will separate from the user's face, allowing much greater leakage to occur. Similarly, at sufficiently low mask pressure relative to ambient, the face seal will tend to buckle, also resulting in large amounts of leakage.

An electrical system exhibiting these properties is shown in figure 22.3. The linear resistors  $R_{\ell 1}$  and  $R_{\ell 2}$  represent seal leakage under normal mask operating conditions; for positive mask pressures (exhalation), diode  $D_2$  is open, allowing a flow out of the mask whose magnitude is dependent on the value of  $R_{\ell 2}$ , while for negative mask pressures (inhalation) diode  $D_1$  is open, and the amount of leakage into the mask depends on the value of  $R_{\ell 2}$ . The pressure source  $P_{\ell e}$  represents the positive mask pressure at which the seal will break away from the user's face; if this pressure is exceeded, diode  $D_4$  opens, and there is additional flow out of the mask through  $R_{\ell 4}$ . In a similar manner, if the mask pressure drops below  $-P_{\ell i}$ , representing the pressure level at which the mask seal will buckle, diode  $D_3$  opens, and flow is allowed into the mask through  $R_{\ell 3}$ .

The block labeled "PORTS" in figure 22.3 contains linear resistors to represent the openings in the mask that house inhalation and exhalation valves. For simplicity, resistance to flow due to any air passages within the mask is lumped together with the port resistance.

The block labeled "PORTS" in figure 22.3 contains linear resistors to represent the openings in the mask that house inhalation and exhalation valves. For simplicity, resistance to flow due to any air passages within the mask is lumped together with the port resistance.

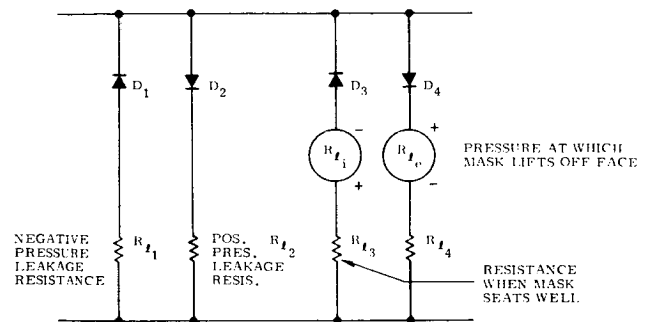


Figure 22.3 Facial seal model.

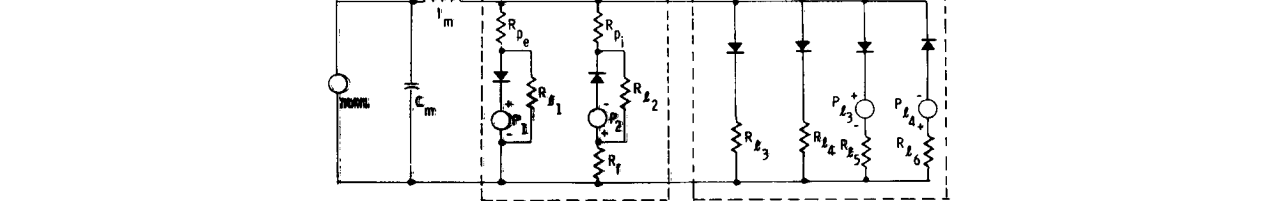


Figure 22.4 Model of filter-type RPD.

## SYSTEMS

### Air Delivery System (ADS)

**Electronic Control Subsystem (ECS<sup>2</sup>).** Any electronic control can be modeled mathematically, where the output equals  $f(\text{input}, t)$ . If the ECS<sup>2</sup> is linear, a transfer function can be used.

**Air Passage Subsystem (APS<sup>2</sup>).** Air passages have their analogy in transmission lines, with distributed parameters of the resistance, inertance and compliance. In most cases, inertance and compliance will be negligible.

**Valve Control Subsystem (VCS<sup>2</sup>).** Valves are modeled as resistances. Simple valves such as flap-type valves are modeled as in figure 22.4 where  $R_L$  is leakage resistance,  $R_p$  is port resistance, and  $P$  is pressure at which valve opens. Valve control is described with transfer functions, as is the ECS<sup>2</sup>.

## Environmental Maintenance System

*Environment Supply Subsystem (ES<sup>3</sup>).* The model of a supply cylinder used here is a pressure source. A breathing bag is normally at 1 atm when partially full and is modeled as a 1 atm pressure source in that state. When empty it has no effect and when full it has the characteristics of a charged parallel compliance and inertance. A heat exchanger is modeled as a resistance.

*Pressure and Venting Subsystem (PVS<sup>2</sup>).* A demand regulator is modeled as a biased diode, where the value of bias is equal to the opening pressure of the demand valve. It is returned to ground, but is understood to be a supply of "good" air. A constant pressure regulator is modeled as a zener diode. Blower systems are referred to as supplementary pressure sources and are modeled as such.

*Air Reconditioning Subsystem (ARS<sup>2</sup>).* Water removal, carbon dioxide scrubber, filters, and heat exchanger are modeled as resistances unless they are active components. If these are flexible components or very large, compliance or inertance or both must be included.

As an example of the modeling process, an air-purifying RPD is shown in figure 22.4. For this system the ADS consisted only of valves and the EMS consisted only of a filter ( $R_1$ ). Since the capacitance of the filter was very small it was not included in the model, nor was the operating time of the valves.

Using electrical circuit analysis simplifications, the model diagram reduces to a simple three-component system with a single compliance, inertance, and resistance. In addition there are a number of valve activating pressures specified that merely change the value of resistance,  $R_{eq}$ , when valves open and close or seal resistance changes. The two state variables for a filter type system are  $Q_I$  and  $P$ . System state equations are

$$\dot{P} = \frac{q_s - Q_I}{C}$$

$$\dot{Q}_I = \frac{P - R_{eq} Q_I}{I}$$

Diode states are determined by the pressure ( $P_R$ ) across the valves calculated from the equation  $\dot{P}_R = \dot{Q}_I R_{eq}$ . This equation was written in differential rather than algebraic form to acknowledge the physical fact that the opening or closing of valves, which are modeled as step changes in  $R$ , can cause instantaneous changes in the rate of change of  $P_R$ , but not in  $P_R$  itself. These differential equations were integrated in a digital computer using a fourth-order Runge-Kutta integration algorithm. Parameters for several different types of mask models were measured as previously discussed and are given in table 22.2.

To check the validity of the modeling, the physical system and the computer model must be driven with similar input functions and their outputs compared.

**Table 22.2** Values of model components as determined for four RPDs.

Mask \ Units	Resistance $Q = 1 \text{ liter/sec}$		Capacitance	Inertance
	Inhalation [cm H <sub>2</sub> O/(liters/sec)]	Exhalation	cm <sup>3</sup> /cmH <sub>2</sub> O	cm H <sub>2</sub> O sec <sup>2</sup> /liter
A	3	1.2	4	0.039
B	4.4	1.85	0.76	—
C	1.5	1.50	2.1	0.00984
D	2.9	0.85	3.3	—

The test function used was generated by a human subject breathing into the test mannequin through a flowmeter. The breathing flow and the pressure in the mask were recorded on a strip chart recorder. These curves were modeled mathematically as piecewise-linear functions with enough data points to insure that the important characteristics of the functions were preserved. The flow curve was then used as the driving function for the computer model.

The important quantity in the evaluation of the dynamic performance of a respiratory protective device is the mask pressure, which is represented here by  $P_R$ , the pressure drop across the valves and filters. Therefore, the model performance criterion chosen was  $(P_{EXP} - P_R)$  where  $P_{EXP}$  is mask pressure measured while the subject was breathing.

The graphs in figures 22.5, 22.6, 22.7, and 22.8 depict the driving function, the experimentally determined pressure, the pressure of the simulated model, and the relative error, respectively. As can be seen, the general shape of the two pressure curves is quite similar. The error curve shows roughly 10 percent disagreement. The large peaks in the error curve are associated with errors in

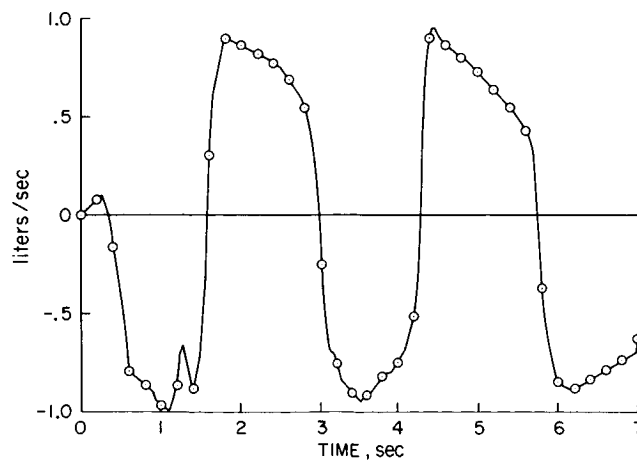


**Figure 22.5** Breathing flow pattern driving both test RPD and computer simulation.

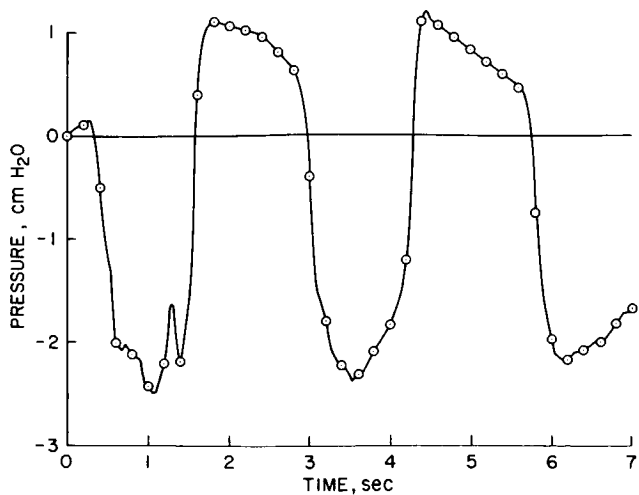


Figure 22.6 Mask pressure as measured for Army M-17 system with driving function of figure 22.5.

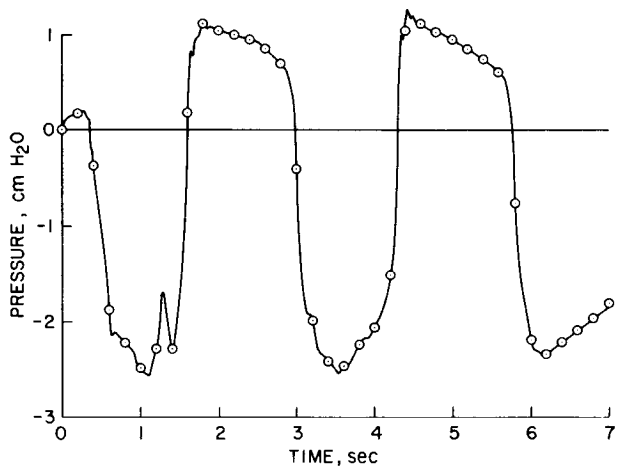


Figure 22.7 Mask pressure as calculated from computer simulation of Army M-17 with driving function of figure 22.5.

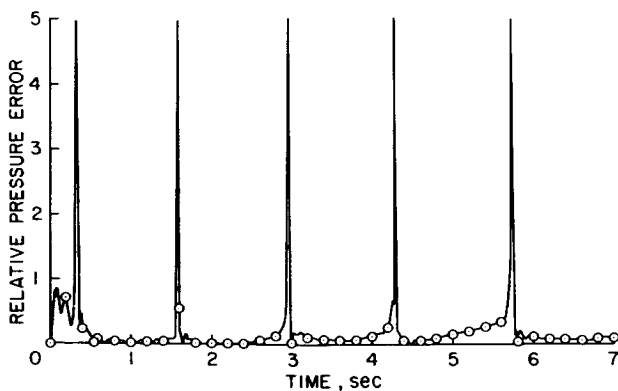


Figure 22.8 Relative error ( $P_{MEAS} - P_{CAL}$ ) of computer simulation of Army M-17 RPD.

reading time visually from the strip chart in regions of large slope. The fact that there are no regions of higher disagreement seems to indicate that the error in the physical measurements of  $I$ ,  $C$ , and  $R$  are a substantial part of the error, as is the error due to transferring data from the strip chart recording.

Values of sensitivity to errors in parameter measurements for  $R$ ,  $C$ , and  $I$  during both inhalation and exhalation are shown in figures 22.9 through 22.14. The quantities graphed are the magnitude of the expressions  $Y(s)$  of the form

$$\frac{\partial P(s)}{\partial x} = Y(s)P(s)$$

where  $P(s)$  is the transform of pressure and  $x$  is the pertinent parameter. Percentage changes in pressure due to given percentage changes in  $x$  are

$$\left| \frac{\Delta P(s)}{P(s)} \right| = x \left| Y(s) \right| \frac{\Delta x}{x}$$

Peak sensitivities are given on each graph.

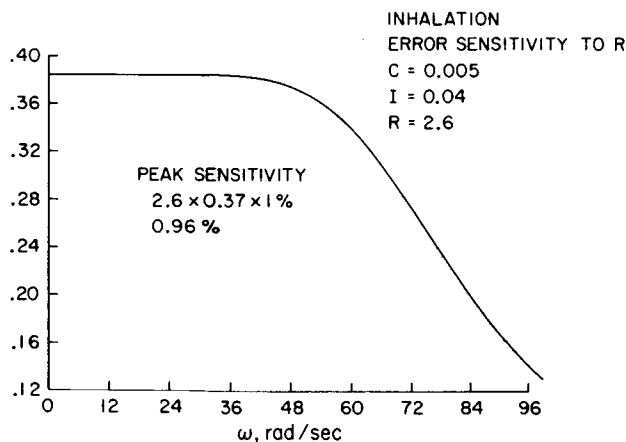


Figure 22.9 Sensitivity of Army M-17 simulation to  $R$  during inhalation.

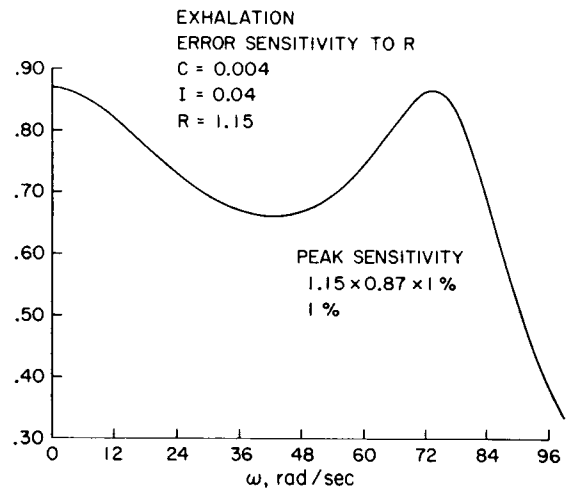
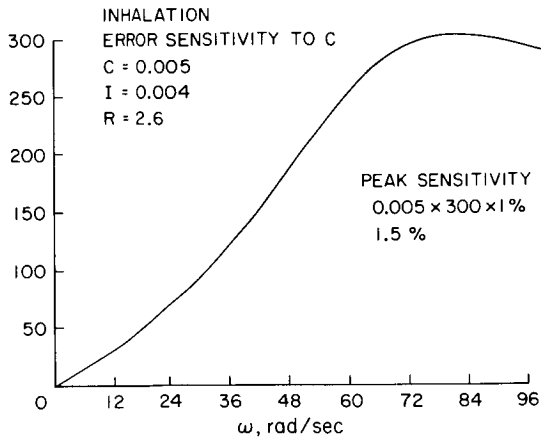
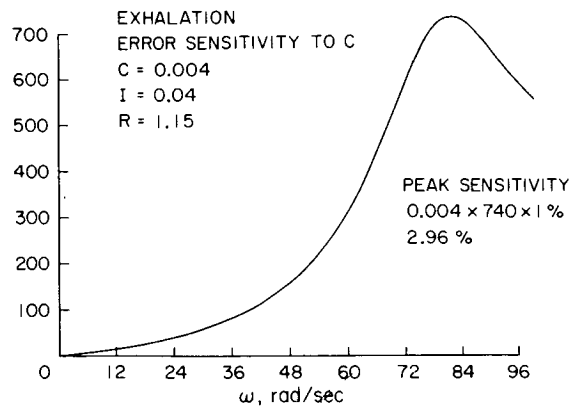


Figure 22.10 Sensitivity of Army M-17 simulation to  $R$  during exhalation.

Much has been learned about the problems of physical measurements of RPDs and refinements will certainly reduce present errors. Also, much improvement in data handling, such as the use of an A to D converter directly to tape for computer use, will be a much more accurate way of evaluating the model. Furthermore, more data will indicate statistically the range over which the models are valid. Completion of this work should provide the RPD Engineer with a valuable analytical engineering tool.



**Figure 22.11** Sensitivity of Army M-17 simulation to C during inhalation.



**Figure 22.12** Sensitivity of Army M-17 simulation to C during exhalation.

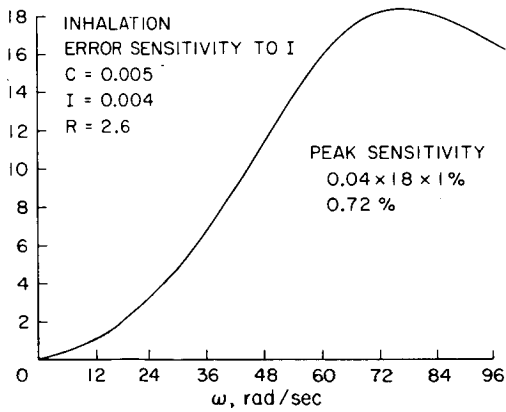


**Figure 22.13** Sensitivity of Army M-17 simulation to I during inhalation.

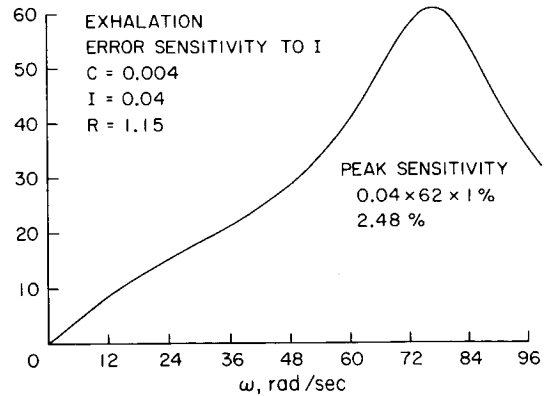


**Figure 22.14** Sensitivity of Army M-17 simulation to I during exhalation.